Environmental and Molecular Mutagenesis 55:103–113 (2014)

Research Article

Copy Number Variants Are Produced in Response to Low-Dose Ionizing Radiation in Cultured Cells

Martin F. Arlt,[1]* Sountharia Rajendran,[1] Shanda R. Birkeland,[2] Thomas E. Wilson,[1,2] and Thomas W. Glover[1,2]

[1]*Department of Human Genetics, University of Michigan, Ann Arbor, Michigan*
[2]*Department of Pathology, University of Michigan, Ann Arbor, Michigan*

Despite their importance to human genetic variation and disease, little is known about the molecular mechanisms and environmental risk factors that impact copy number variant (CNV) formation. While it is clear that replication stress can lead to de novo CNVs, for example, following treatment of cultured mammalian cells with aphidicolin (APH) and hydroxyurea (HU), the effect of different types of mutagens on CNV induction is unknown. Here we report that ionizing radiation (IR) in the range of 1.5–3.0 Gy effectively induces de novo CNV mutations in cultured normal human fibroblasts. These IR-induced CNVs are found throughout the genome, with the same hotspot regions seen after APH- and HU-induced replication stress. IR produces duplications at a higher frequency relative to deletions than do APH and HU. At most hotspots, these duplications are physically shifted from the regions typically deleted after APH or HU, suggesting different pathways involved in their formation. CNV breakpoint junctions from irradiated samples are characterized by microhomology, blunt ends, and insertions like those seen in spontaneous and APH/HU-induced CNVs and most nonrecurrent CNVs in vivo. The similarity to APH/HU-induced CNVs suggests that low-dose IR induces CNVs through a replication-dependent mechanism, as opposed to replication-independent repair of DSBs. Consistent with this mechanism, a lower yield of CNVs was observed when cells were held for 48 hr before replating after irradiation. These results predict that any environmental DNA damaging agent that impairs replication is capable of creating CNVs. Environ. Mol. Mutagen. 55:103–113, 2014.

Key words: CNV; ionizing radiation; replication stress

INTRODUCTION

Copy number variants (CNVs), defined as deletions or duplications of 50 bp to over a megabase, play a major role in human genetic variation and disease [Zhang et al., 2009]. Despite their importance, little is known about the genetic and environmental risk factors that impact CNV formation. Replication stress caused by aphidicolin (APH) and hydroxyurea (HU) has been shown to induce a high frequency of de novo CNVs in cultured human and mouse cells that arise in a NHEJ-independent manner and mimic a subclass of human nonrecurrent CNVs in size and breakpoint structures [Durkin et al., 2008; Arlt et al., 2009, 2011b, 2012]. There is also a measurable frequency of spontaneous CNV formation in untreated cells, indicating that replication errors produce these lesions during normal cell division. Many APH- and HU-induced CNVs map within hotspots, regions in which multiple overlapping CNVs arose independently in different cells, including hotspots observed in known chromosomal common fragile site regions, like FRA16D in *WWOX* and the fibroblast fragile site at 3q13.31 [Arlt et al., 2011b]. Some hotspots correlate with clinically relevant CNV regions, including *AUTS2*, which has similar CNVs in patients with autism and other neurodevelopmental disorders [Glessner et al., 2009; Beunders et al., 2013], *MAGI2*, which is implicated in bipolar disorder [Karlsson et al., 2012], and a 3q13.31 hotspot, which is frequently

Additional Supporting Information may be found in the online version of this article.

Grant sponsor: NIEHS; Grant number: RCI-ES018672 (T.W.G. and T.E.W.).

*Correspondence to: Martin F. Arlt, Department of Human Genetics, 4909 Buhl, Box 5618, 1241 E. Catherine Street, University of Michigan, Ann Arbor, MI 48109-5618. E-mail: arltm@umich.edu

Received 16 October 2013; provisionally accepted 26 November 2013; and in final form 27 November 2013

DOI 10.1002/em.21840

Published online 10 December 2013 in Wiley Online Library (wileyonlinelibrary.com).

deleted in primary osteosarcomas and cancer cell lines [Kresse et al., 2009; Bignell et al., 2010; Pasic et al., 2010].

While it is clear that replication inhibitors can lead to de novo CNVs, the effect of different types of mutagens on CNV induction is unknown. Here, we examine ionizing radiation (IR) for its effects on CNV formation in cultured normal human fibroblasts. IR is a DNA-damaging agent generated by both natural and man-made sources that induces several types of DNA damage in the cell, including double strand breaks (DSBs), single-strand breaks (SSBs), and base damage [Helleday et al., 2007]. DSBs are a particularly deleterious lesion that, if left unrepaired or are misrepaired, can lead to genomic instability and cell death. In addition, if a replication fork encounters a SSB, the fork can collapse into a one-sided DSB [Kuzminov, 2001]. Because IR creates roughly 20 times more SSBs than DSBs, SSBs are a frequent form of damage that can potentially interfere with replication [Ward, 1988].

We report here that IR in the range of 1.5–3.0 Gy results in a significant increase in de novo CNV formation over unirradiated cells. The IR-induced CNVs are found throughout the genome, with many of the same hotspot regions seen after APH- and HU-induced replication stress, and including a novel hotspot at the *CDKN2A* (p16) tumor suppressor gene, which is deleted in many cancers [Kohno and Yokota, 2006]. The CNV breakpoint junctions are characterized by microhomologies, blunt ends, and insertions like those seen in spontaneous and replication stress-induced CNVs and most nonrecurrent CNVs in vivo. Interestingly, IR produces a higher proportion of duplications than do APH and HU and, at most hotspots, these duplications are shifted in location from the regions typically deleted after replication stress. CNV induction was eliminated when cells were allowed to recover before replating to generate clones. We also observed differences in IR-induced CHK1 phosphorylation after cells were irradiated and either allowed to recover or immediately trypsinized and plated for clonal expansion. These data suggest that low-dose IR induces CNVs through a replication-dependent mechanism, as opposed to via replication-independent repair of DSBs.

MATERIALS AND METHODS

Cell Line and Culture Conditions

All experiments were performed with an hTERT-immortalized derivative of normal human fibroblast cell line HGMDFN090 (090), which was obtained from the Progeria Research Foundation (Peabody, MA) and previously described [Arlt et al., 2009]. The source individual is a female of European descent with a normal 46, XX karyotype. Cells were grown in DMEM media supplemented with 15% FBS. The starting cell population was an expansion of a single cell-derived clone, to minimize the effect of preexisting mosaic CNVs in the cell line.

The cells were seeded onto T25 flasks the day before irradiation and the media was changed the following day, before irradiation. Irradiations were carried out on cells in exponential growth phase using a Philips RT250 (Kimtron Medical) at a dose rate of approximately 2 Gy/min in the University of Michigan Comprehensive Cancer Center Experimental Irradiation Core. After irradiation, clonal expansions of 090 were generated as described previously [Arlt et al., 2009]. Briefly, after treatment, cells were plated at a density of 100–500 cells per 100-mm culture dish. After 7–10 days, individual clones were isolated from these plates using cloning rings and serially expanded in 6-well plates and culture flasks. In the first and second experiments, cells were trypsinized and plated at a low density for clones, immediately after radiation. In the third experiment, irradiated cells were allowed to recover for 48 hr before being trypsinized and plated for clones. Cells were plated at a density of 100–2000 cells per 100-mm culture dish and individual clones isolated using cloning rings after 10–14 days. Genomic DNA was prepared from cell lines using the Blood & Cell Culture DNA Mini Kit (Qiagen).

SNP Microarrays

CNVs were detected using the 1M feature Illumina HumanOmni1-Quad BeadChip and Illumina HumanOmni2.5-8, which have both SNP and non-SNP probes, as well as Nimblegen 12 × 270K genomic aCGH arrays. Illumina arrays were run by the University of Michigan DNA Sequencing Core, including determination of probe log R ratios and B allele frequencies. Genomic aCGH on Nimblegen arrays was performed according to manufacturer's instructions, using the clonal starting cell population as a reference DNA. De novo CNV detection was performed using our software platform, VAMP, exactly as previously described [Arlt et al., 2011a, 2011b]. For illumina arrays, de novo CNVs were detected by comparing probe intensities and B allele frequencies for each test sample array to an array run on the clonal starting cell population. De novo CNVs were detected in Nimblegen arrays by a change in probe intensity between test and reference samples on each array. This approach routinely detects CNVs larger than 20 kb and can detect CNVs as small as a ~1 kb depending on probe placement.

Mate Pair Sequencing

Genomic DNA (20–25 μg) was used to construct mate-pair libraries using the Illumina Mate Pair Library Prep Kit followed by paired end sequencing by the University of Michigan DNA Sequencing Core according to the manufacturer's instructions. Analysis of read pair data proceeded exactly as described in Birkeland et al. [2010]. Briefly, reads were mapped to the hg18 reference genome and de novo structural variants were identified by seeking sets of anomalously mapping fragments, followed by visual inspection to confirm that multiple read pairs identified the same putative variant in the treated clone but not in a paired library prepared from untreated 090 cells.

CNV Breakpoint Junctions

For deletions, PCR primer pairs were generated that flanked deletion breakpoints, whereas for duplications, primers were designed within the duplicated region, directed outward, as described previously [Arlt et al., 2009]. PCR using the Expand Long Template PCR System (Roche Applied Science) generated a product that spanned the breakpoint junction. All products were then subjected to standard Sanger sequencing and compared to the reference genome (build hg19) to determine breakpoint junctions.

Statistical Methods

CNVs in our model system are relatively rare events and, therefore, the numbers of CNVs per clone are expected to fit a Poisson distribution

determined by the mean frequency of CNVs in all clones. Therefore, *P* values of treated versus untreated samples were determined using the one-sided *E*-test of Krishnamoorthy and Thomson for comparing two Poisson mean rates [Krishnamoorthy and Thomson, 2004]. Simulation analyses were performed as described previously for APH and HU CNVs [Arlt et al., 2011b]. The non-parametric Kolmogorov–Smirnov test (http://www.physics.csbsju.edu/stats/KS-test.n.plot_form.html) was used to analyze the potential difference in CNV size spectra between IR-treated and APH/HU-treated clones.

Western Blotting

Cell lysates were prepared by resuspending cell pellets in SDS-lysis buffer followed by sonication. 10% Bis-Tris gels were used to resolve proteins. Whole-cell lysate (40 μg) was loaded per lane. Gels were transferred to PVDF membrane (Millipore) using a Trans-Blot SD Semi-Dry Transfer system (Bio-Rad Laboratories). Antibody hybridization and chemiluminescence detection were performed according to standard protocols. CHK1 protein was detected with sc-8408 (Santa-Cruz Biotechnology). CHK1 phosphorylation on Ser317 was detected with Phosho-Chk1 (Ser317) (Cell Signaling). Tubulin was detected with Ab-2 DM1A (Thermo Scientific). HRP-conjugated anti-mouse and anti-rabbit antibodies were obtained from GE Healthcare, Piscataway. Protein bands were quantitated using ImageJ software [Rasband, 1997].

RESULTS

Ionizing Radiation Induces De Novo CNVs in Human Fibroblasts

Subconfluent normal hTERT-immortalized human fibroblasts were irradiated immediately prior to trypsinization and plating for clones. Fifteen-independent, expanded clones each from cell populations treated with 0, 0.5, 1.0, and 1.5 Gy were subjected to CNV analysis using Illumina 1M SNP arrays. Untreated clones had a low frequency of 0.67 de novo CNVs per clone, similar to previously observed frequencies of spontaneous CNV mutations in these cells [Arlt et al., 2011b]. The frequency of de novo CNVs increased with higher doses of radiation. Cells exposed to 1.5 Gy had 1.80 de novo CNVs per clone, a significant ($P = 0.0024$) increase in de novo CNV formation compared to untreated controls (Fig. 1a). These cells displayed a marked decrease in colony-forming ability (Fig. 1b).

This experiment was repeated using doses of 0, 1.5, and 3.0 Gy with similar results. Untreated clones showed the expected low level of spontaneous CNV induction (0.58 CNVs per clone; $n = 12$) while cells exposed to 3.0 Gy IR had a significant increase to 1.86 ($P = 0.0016$; $n = 14$) de novo CNVs per clone, as well as a reduction in survival (Figs. 1c and 1d).

De novo CNVs from the combined experiments were a mix of both deletions and duplications, with a slight excess of copy number gains over losses. Ten of 17 (59%) spontaneous CNVs arising in untreated cells were duplications. This gain/loss ratio did not change substantially in IR-treated cells, in which 47 of 92 (51%) CNVs were duplications. This is a higher ratio of gains to losses than previously seen in APH- and HU-induced CNVs, in which 64 of 216 (30%) CNVs were gains.

There was no difference in de novo CNV size distribution between untreated and irradiated cells (Fig. 2a). Spontaneous, de novo CNVs in untreated cells were generally large, with a median size of 261 kb (22.3 kb to 15.0 Mb). IR-induced CNVs had a similar median size of 288 kb (2.7 kb to 34.2 Mb). We did note that IR-induced CNV size distribution shifted slightly larger than observed previously for CNVs induced by APH or HU, which showed a median size of 137.3 kb, less than half that seen in IR-induced CNVs (Fig. 2b) [Arlt et al., 2011b]. However, a Kolmogorov–Smirnov test showed no significant difference in the size spectra of CNVs in these two groups ($P = 0.124$) (Supporting Information Fig. S1).

Some forms of structural variants, including some types of complex rearrangements and events that do not change copy number, such as inversions, cannot be detected using array-based approaches. To determine if such events occur frequently after IR, two irradiated clones, 1CX1.5A41 and 1CX1.5A33 were further analyzed for de novo CNV content using mate pair sequencing as previously described [Arlt et al., 2011a]. This approach recapitulated the CNVs detected using arrays, but did not reveal the presence of any additional rearrangements, suggesting that large CNVs are the primary chromosomal anomaly formed after low-dose IR in these cells.

Genomic Distribution of IR-Induced CNVs

Spontaneous and IR-induced CNVs were distributed throughout the genome, with most arising in distinct, nonoverlapping regions (Fig. 3a). Superimposed on this distribution pattern were hotspots containing more than three overlapping CNVs. Hotspots accounted for 19.7% (25/127) of all CNVs, a lower proportion than has been seen with replication stress (~35%), although we had scored twice as many APH/HU-induced CNVs than IR-induced CNVs (216 vs. 105, respectively), making replication stress clusters easier to detect [Arlt et al., 2011b]. Each CNV within the IR-induced hotspots had unique boundaries, indicating that each arose as an independent event. Notably, these hotspots corresponded to the CNV hotspots seen when cells are grown under conditions of replication stress induced by APH or HU [Arlt et al., 2011b]. As with APH and HU, de novo CNVs were most frequently observed at 3q13.31 near *LSAMP* and at 7q11.22 within *AUTS2*. One to three de novo CNVs in IR-treated clones were found at previously defined hotspots at 1q44 (*KIF26B, SMYD3*), 10q11.23-q21.1 (*PRKG1*), and 16q23.1 (*WWOX*) [Arlt et al., 2011b]. In addition to these previously defined hotspots, a new hotspot was found at 9p21.3, a region containing the *CDKN2A* (p16) tumor suppressor gene. This locus is frequently deleted in many cancers with breakpoint junction characteristics similar to those observed in our de

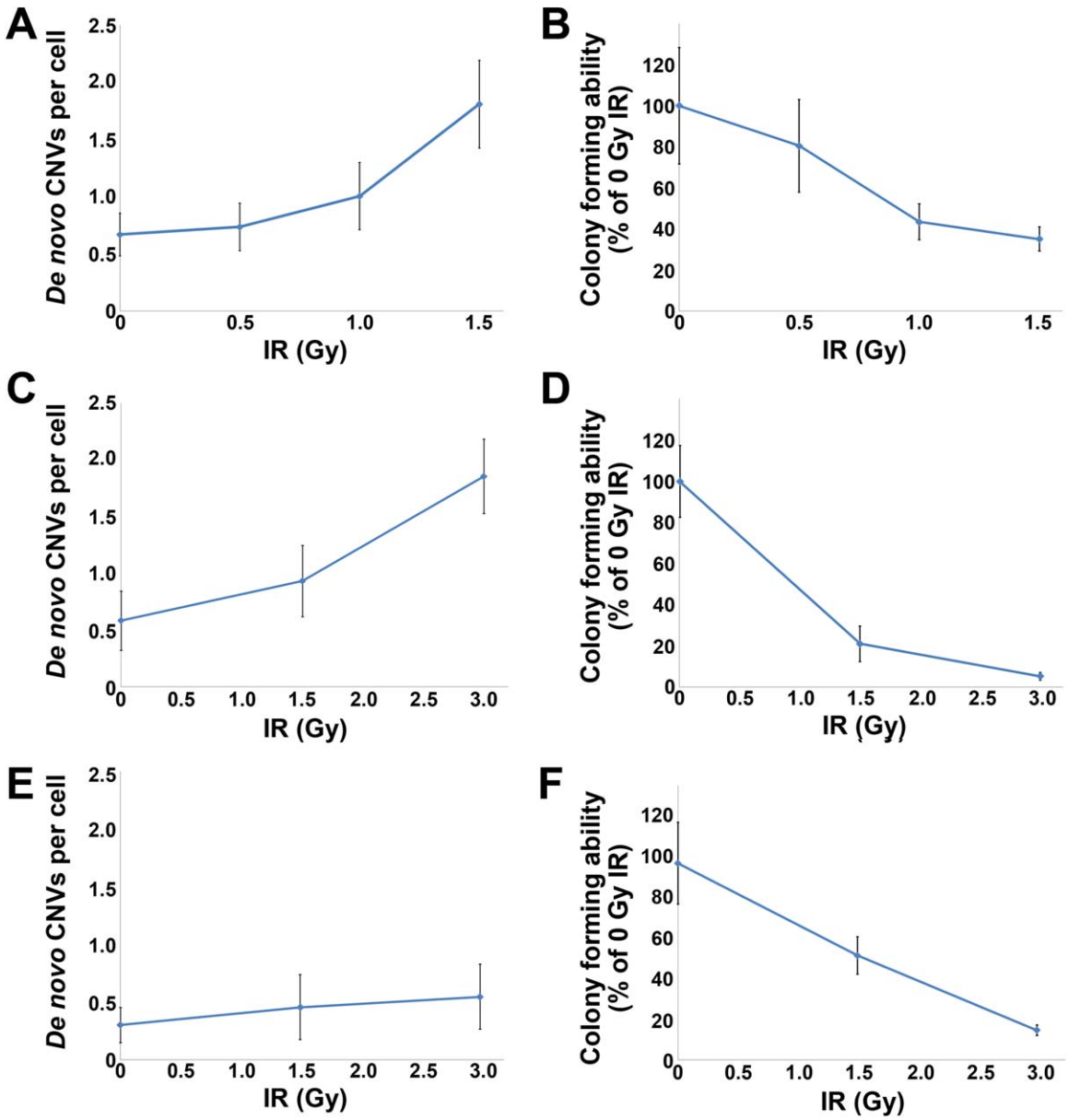

Fig. 1. IR induces de novo CNVs in normal human fibroblasts. Three iterations of the experiment with different cell handling are shown. (**A**) Incidence of de novo CNVs in normal, hTERT-immortalized human fibroblasts treated with 0-1.5 Gy IR. Fifteen independent clones each of untreated, 0.5 Gy, 1.0 Gy, and 1.5 Gy-treated cells were analyzed. Cells were plated for cloning immediately after irradiation. Error bars indicate SE. (**B**) Colony-forming ability of IR-treated cells in (A) compared to untreated cells. Error bars indicate SD. (**C**) Incidence of de novo CNVs in normal, hTERT-immortalized human fibroblasts treated with 0–3.0 Gy IR. Twelve independent clones of untreated cells, 15 clones of 1.5 Gy, and 14 clones of 3.0 Gy-treated cells were analyzed. Cells were plated for cloning immediately after irradiation. Error bars indicate SE. (**D**) Colony-forming ability of IR-treated cells in (C). (**E**) Incidence of de novo CNVs in normal, hTERT-immortalized human fibroblasts treated with 0–3.0 Gy IR. Ten independent clones of untreated cells and 11 clones each of 1.5- and 3.0-Gy-treated cells were analyzed. Unlike (A) and (C), cells in (E) were plated for cloning 48 hr after irradiation. Error bars indicate SE. (**F**) Colony-forming ability of IR-treated cells in (E) compared to untreated cells. Error bars indicate SD. [Color figure can be viewed in the online issue, which is available at wileyonlinelibrary.com.]

novo CNVs [Kohno and Yokota, 2006]. This site had not been previously defined as a replication stress-induced CNV hotspot, although two APH/HU-induced CNVs were seen at this locus in human fibroblasts [Arlt et al., 2011b].

We used a simulation to determine whether IR-induced CNVs were nonrandomly associated with APH- and HU-induced CNV regions. Our set of IR CNV regions was randomly placed around the genome in 10,000 permutations and then compared to the locations of replication stress-induced CNV regions to create an expected random distribution of overlap between the two groups. In addition, a single iteration was mapped in which the IR CNVs regions were offset 10 Mb to the right. These results were compared to the observed IR CNV locations

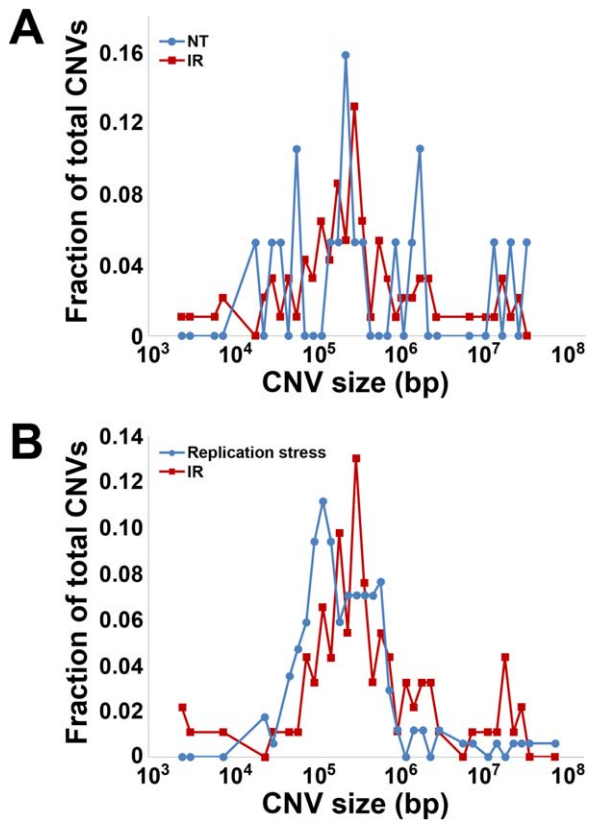

Fig. 2. Size distribution of CNVs. (**A**) Fraction of CNVs by size. Untreated (blue circles), IR-treated (red squares). (**B**) Fraction of CNVs by size for CNVs induced by APH and HU (blue circles) [Arlt et al., 2011b] and IR (red squares). [Color figure can be viewed in the online issue, which is available at wileyonlinelibrary.com.]

(Fig. 4). The spatially shifted CNV regions did not overlap APH/HU-induced CNVs more than expected by chance. In contrast, there was a significant enrichment after IR for previously mapped CNVs for both regions where two or more CNVs mapped ($P = 3.3 \times 10^{-6}$) and singleton CNVs ($P = 0.0024$).

We noted that IR appears to induce duplications versus deletions at a higher relative frequency than APH or HU. We further noted that, while CNV hotspot locations were correlated after IR and APH/HU, the type of CNVs in these hotspots often differed. Specifically, the hotspot in *AUTS2* at 7q11.22 was found to contain CNVs primarily of the deletion type (10/11, 91%) after APH and HU [Arlt et al., 2011b], whereas after IR this hotspot had almost exclusively duplication CNVs (9/10, 90%) (Fig. 3B). A similar pattern was seen at *WWOX* at 16q23.1, where 6/6 replication stress-induced CNVs were deletions, and 3/3 IR-induced CNVs were duplications (Fig. 3b). Importantly, at both of these hotspots it was further observed that most of the duplication CNVs observed with IR were shifted in location relative to the region of deletion CNVs observed with replication stress. Not all hotspots followed this altered pattern. For example, the 3q13.31 hotspot contained almost exclusively deletions that occurred within the same genome span after both IR (9/9, 100%) and APH/HU (29/31, 94%) [Arlt et al., 2011b].

We observed three very large CNVs (2 deletions, 1 duplication) that were 15-22 Mb in size that involved gain or loss of material extending distally to the chromosome end. It is likely that such large, terminal CNVs arise via a DSB-repair mechanism different than that giving rise to the majority of the smaller observed CNVs. In addition to CNVs, three clones exhibited long, 27–35 Mb stretches of loss of heterozygosity (LOH) extending to the terminus of chromosome 9p (Supporting Information Fig. S2). These regions displayed a change in the B-allele frequency of SNPs across the region, but no corresponding change in the Log *R* ratio, indicating no change in copy number. In addition, these events were mosaic within the clonal population, indicating they occurred after cells had been replated for single cell cloning. As they did not affect copy number, these rearrangements are not included in the CNV totals.

Characterization of IR-Induced CNV Breakpoint Junctions

Previous work has demonstrated that nonrecurrent CNVs in vivo and replication stress-induced CNVs in cultured cells have breakpoint junctions that are primarily characterized by short stretches of microhomology, blunt ends, or small insertions, as opposed to long stretches of homology that would indicate homologous repair in their formation [Arlt et al., 2009, 2011b, 2012; Zhang et al., 2009]. To explore the mechanism of IR-induced CNV formation, we examined 18 CNV breakpoint junctions from 17 de novo CNVs in IR-treated cells (Table I; Fig. 5a). Two breakpoints (11.1%) were characterized by blunt ends and 14/18 (77.8%) had short (1–8 bp) stretches of microhomology. The remaining two breakpoints (11.1%) each lacked microhomology and contained a single base insertion resulting from polymerase slippage, similar to insertions seen in APH/HU-induced CNVs and in vivo [Arlt et al., 2011b, 2012; Carvalho et al., 2013]. These breakpoint characteristics are the same as those seen in spontaneous and APH/HU-induced CNVs observed previously [Arlt et al., 2009, 2011b, 2012]. Two of these CNV junctions were from a single, complex CNV (Fig. 5b). This CNV consisted of 97.7 kb deletion with an ectopic insertion of 530 bp of sequence whose origin was 4.8 kb upstream of the deletion. This rearrangement is very similar in organization to complex CNVs induced by APH and HU in both human and mouse cells [Arlt et al., 2011b, 2012].

We were successful in sequencing the breakpoint junctions from 65.4% (17 of 26) of attempted CNVs. None of the de novo CNVs in our experiments were characterized by segmental duplications or other long stretches of

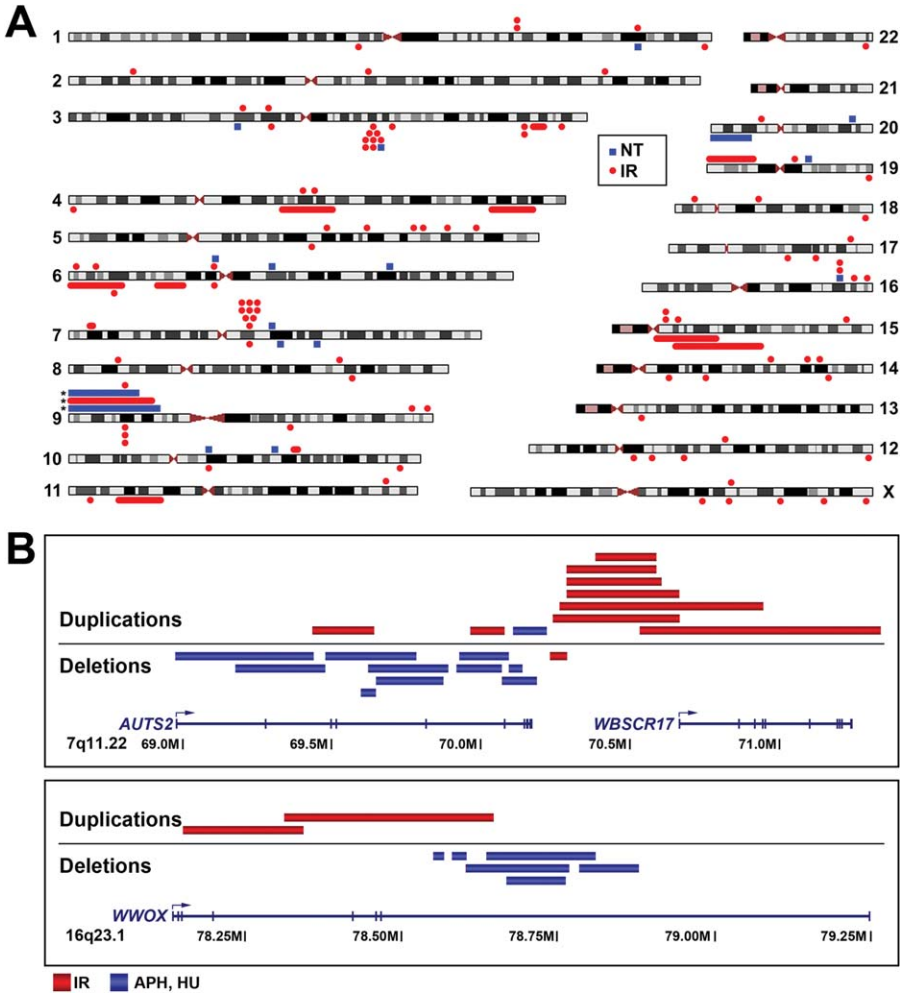

Fig. 3. Spatial distribution of CNVs. (**A**) Locations of IR-induced CNVs. Red circles indicate IR-induced CNVs, blue squares indicate spontaneously arising CNVs in untreated cells. Bars are used to indicate large CNVs spanning more than a chromosomal band. Markers above and below chromosomes represent duplications and deletions, respectively. Asterisks (*) mark three large regions of uniparental disomy on chromosome 9p. Ideograms were adapted from the University of California, Santa Cruz genome browser (http://genome.ucsc.edu) [Kent et al., 2002]. Precise coordinates for all de novo CNVs are listed in Dataset S1. (**B**) Examples of physically shifted hotspot CNVs after IR (red bars) and APH/HU (blue bars). In addition, CNVs induced by IR in these regions are predominantly duplications whereas those induced by APH/HU are mostly deletions.

homology at or near the breakpoint regions in the reference genome sequence that would indicate the involvement of homologous recombination in their formation. The CNVs for which breakpoint cloning failed likely represent junctions with complex structures that are difficult to amplify, even using multiple primer sets flanking the breakpoints. Therefore, we expect that our single complex CNV is an underrepresentation of the actual incidence of complex events in our samples.

Postirradiation Recovery Eliminates IR-Induced CNV Formation

It is known that trypsinizing irradiated fibroblasts causes them to immediately resume DNA replication and reenter the cell cycle [Gadbois et al., 1997]. Given that IR-induced CNVs matched APH/HU-induced CNVs with respect to size, location, and breakpoint junction characteristics, we hypothesized that trypsinizing and plating cells for clones immediately postirradiation led to IR damage-induced replication stress, which contributed to formation of de novo CNVs. To test this, cells were irradiated as before with 0, 1.5, and 3 Gy, except that the cells were given a 48-hr postirradiation recovery period before being trypsinized and plated for clone isolation. We analyzed 10 untreated clones and 11 clones each from the 1.5 and 3 Gy treatment conditions for de novo CNVs (Fig. 1e). The untreated clones had a frequency of 0.30 de novo CNVs per clone. In contrast to irradiated cells that were immediately plated for clonal expansion, the irradiated clones given a recovery period did not have a significant change in CNV frequency compared to the

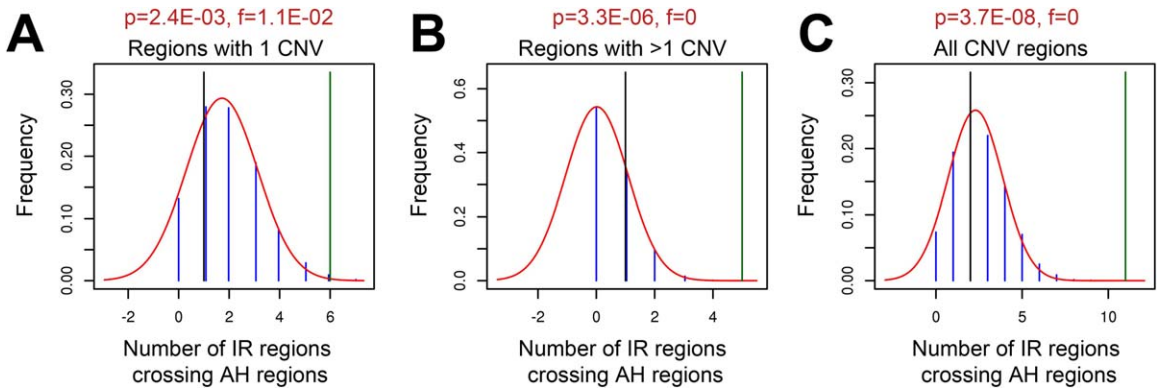

Fig. 4. Non-random association of IR-induced CNVs and APH/HU-induced CNVs. IR CNV regions were randomly distributed around the genome in 10,000 permutations and then compared to the locations of CNV regions induced by APH and HU (AH) to create an expected random distribution of overlap between the two groups. The actual observed number of IR CNV regions that overlapped AH CNV regions is indicated by the vertical green line. The black line represents a single iteration in which the IR CNV regions were offset 10 Mb to the right. Blue lines and associated red Gaussian curve-fit show the distribution of values observed for the 10,000 random permutations. Analyses were performed for (**A**) singleton IR CNVs, (**B**) regions with more than one IR CNV, and (**C**) all IR CNV regions combined. Numbers in red above each plot indicate the *P*-value for the actual value calculated from the fit curve (*P*), as well as the cumulative frequency of iterations that had as many or more IR CNV regions crossing AH regions as the actual value (*f*). [Color figure can be viewed in the online issue, which is available at wileyonlinelibrary.com.]

TABLE I. Breakpoint Junctions of IR-Induced CNVs

Clone	[IR] (Gy)	CNV type	Chr	Left breakpoint (hg19)	Right breakpoint (hg19)	# bp homology at junction	Homologous bases	Inserted bases
1CX1B23	1.0	Deletion	4	81,026,798	101,318,742	2	GT	—
1CX1.5A41	1.5	Deletion	1	85,957,519	85,984,003	0	—	C
1CX1.5A41	1.5	Deletion	2	28,941,965	28,943,397	2	AC	—
15B1	1.5	Deletion	3	114,338,052	114,601,491	8	AA(C/A)ATTTC	—
1CX1.5A41	1.5	Deletion	3	115,588,199	116,192,341	0	—	—
15B1	1.5	Deletion	3	116,729,604	116,627,448	0	—	CC
1CX1.5A41	1.5	Deletion	3	171,827,497	171,974,363	2	TT	—
1CX1.5A33	1.5	Duplication	7	70,574,902	70,205,688	3	TAT	—
1CX1.5A32	1.5	Deletion	10	53,571,361	53,778,026	2	AT	—
1CX1.5B12	1.5	Deletion	14	89,918,224	90,090,047	2	AT	—
1CX1.5A41	1.5	Deletion	17	48,643,949	48,730,887	7	AG(G/A)TCAC	—
3T1	3.0	Deletion	4	161,882,750	178,397,061	1	A	—
3S3	3.0	Duplication	7	70,018,241	69,893,758	2	TG	—
3T2	3.0	Deletion	7	70,154,118	70,224,314	1	G	—
3F1	3.0	Deletion	11	18,376,572	36,717,065	2	GT	—
3D5	3.0	Complex	17	59,126,424	59,228,874	0	—	—
3D5	3.0	Complex	17	59,131,175	59,125,894	3	CCA	—
3C2	3.0	Deletion	19	57,743,180	58,050,665	1	G	—

control, with 0.45 and 0.55 CNVs per clone detected in the 1.5 and 3.0 Gy groups, respectively ($P = 0.285$ and 0.205, respectively). Thus, allowing cells to remain on the plate for a 48-hr recovery period prior to replating for clone isolation suppressed CNV induction by IR. Cells given a recovery period still demonstrated a reduction in survival (Fig. 1f).

To evaluate the effect of post-IR recovery further, we tested cell cycle checkpoint induction following IR, with and without a recovery period. Cells were exposed to 3 Gy, after which they were either immediately trypsinized and replated, or left on the plate to recover. Cell lysates from both groups were harvested at 1, 6, 24, and 48 hr after irradiation. CHK1 phosphorylation on serine 317 was measured by western blot as a measure of checkpoint activation (Fig. 6). Cells that were trypsinized immediately after irradiation showed considerably lower levels of CHK1 activation than cells that were not trypsinized, especially at the earliest time point, consistent with the idea that trypsinization and stimulation of cell division partially suppressed the checkpoint response to IR. In both cases, CHK1 phosphorylation was reduced to background levels within 24 hr after IR. These results are

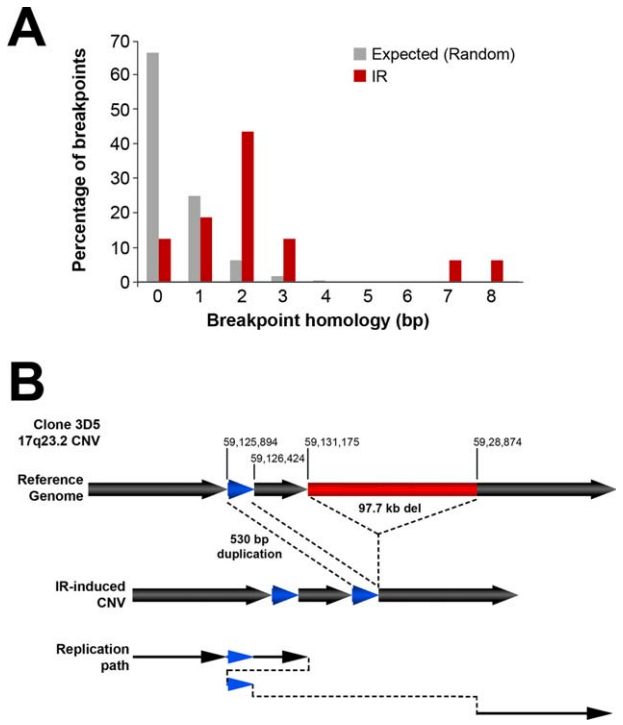

Fig. 5. CNV breakpoint junctions. (**A**) De novo CNV breakpoint junction sequence homology in IR-treated cells (red) compared to the expected distribution if microhomology usage was random (gray). (**B**) A complex CNV with two junctions at 17q23.2 in 3.0-Gy-treated clone 3D5. Based on aCGH data, this CNV was called as a deletion, but sequencing of the breakpoint junctions revealed that this CNV was complex, containing a 97.7 kb deletion (red), as well as a duplication-insertion of 530 bp (blue) at the deletion boundary. [Color figure can be viewed in the online issue, which is available at wileyonlinelibrary.com.]

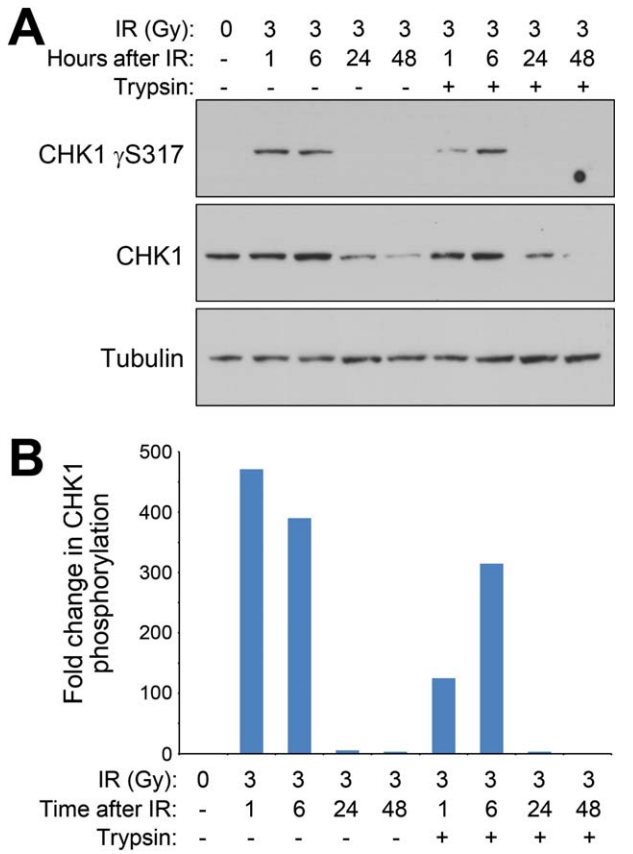

Fig. 6. Immediate trypsinization and replating of cells following IR reduces CHK1 activation. (**A**) Western blots showing the induction by IR of CHK1 phosphorylation on residue S317. (**B**) Quantitation of CHK1 S317 phosphorylation in (A), normalized to tubulin, respectively. [Color figure can be viewed in the online issue, which is available at wileyonlinelibrary.com.]

consistent with protocol-dependent induction of replication stress by low-dose IR.

DISCUSSION

The spectrum of genotoxins and DNA damaging agents that lead to increased rates of CNV formation, and the mechanisms by which these agents might act, are very poorly understood. We have previously demonstrated that at least two chemical agents that cause replication stress via impairment of replication fork progression, APH and HU, induce one type of CNV in a manner consistent with replication-associated models of CNV formation by template switching and microhomology-mediated break-induced repair (MMBIR) [Arlt et al., 2009, 2011b]. Experiments reported here now demonstrate that low-dose IR, a direct DNA damaging agent, induces similar de novo CNVs in cultured normal human fibroblasts. The sizes and breakpoint junction sequences of these IR-induced CNVs are consistent with the nonrecurrent class of de novo pathogenic CNVs, a large class of normal human CNVs. IR-induced CNVs are also very similar to those induced by APH and HU, including the critical observation that they are frequently located within the same hotspot regions.

IR, and by extension possibly other direct DNA damaging agents, might induce CNVs in at least two distinct ways. First, the DSBs that are principally responsible for the cytotoxicity of IR might be the direct substrates of CNV formation via an end joining process. Several factors suggest that this is not the most likely explanation for IR-induced CNVs. It is difficult to reconcile the expected burden of 12–36 DSBs per cell at the IR doses used with the frequency of observed CNVs, which in this model would presumably require two closely separated DSBs. Moreover, if random DSBs were the key intermediate, it is unclear why they would lead to the same non-random genomic distribution of CNVs as replication stress. In particular, it is highly unlikely that IR induces DSBs with a high enough frequency at hotspot loci to explain the CNVs we observed there. In addition, the prevalence of copy number gains is difficult to explain with an end joining repair mechanism. We also note that

classical NHEJ, expected to act in the repair of IR DSBs, has been ruled out as a major factor in CNV formation after replication stress in mouse ES cells [Arlt et al., 2012], although alternate end-joining remains a possible mechanism of formation for at least the deletion CNVs.

In contrast, IR might lead to CNV formation via secondary effects that result from the more abundant non-DSB lesions, including SSBs and base lesions, or from alterations in the cell state leading to altered replication or repair function. Indeed, the clear similarity between IR- and APH/HU-induced CNVs strongly suggests that low-dose IR-induced CNVs result from IR-dependent replication stress and replication errors, as opposed to direct joining of IR-induced DSB ends. A replication-dependent model for CNV induction by IR is further supported by the observation that allowing IR-exposed cells to recover for 48 hr before plating for clonal expansion suppresses IR-induced CNVs. It is well established that after IR exposure at doses as low as 1 Gy, cultured human fibroblasts undergo a seemingly irreversible G1 arrest [Di Leonardo et al., 1994; Gadbois et al., 1996]. This arrest was long thought to be permanent, until it was discovered that if cells are trypsinized and replated, they immediately resume DNA replication and reenter the cell cycle, likely due to the disruption of cell–substrate interactions [Gadbois et al., 1997; Dimitrijevic-Bussod et al., 1999]. In addition, fibroblasts that undergo trypsinization in late G1 have hyperphosphorylated retinoblastoma protein, making them resistant to further cell cycle checkpoint activation as they proceed through S phase [Guadagno and Assoian, 1991].

Consistent with previous results with replication inhibitors, we did not see extensive evidence for an IR-induced increase in copy number neutral LOH. Only three clones, both treated and untreated, showed such events, and all arose on the short arm of chromosome 9, suggesting that there may be something unusual about this chromosomal region. Overall, these observations support the notion that CNVs arise mainly by template-switches and/or DSB mispairings between closely associated regions of replicating chromatids, and not between unassociated and potentially distant homologous chromosomes. The fact that this pattern was not altered by IR also reinforces the idea that CNVs arise mainly by replication-dependent lesions and not by IR-induced DSBs in nonreplicating regions.

The lack of an increase in de novo CNV frequency when IR-treated cells are allowed to recover for 48 hr prior to trypsinization suggests that these cells are faithfully repairing damage prior to reactivated DNA replication. The 48-hr recovery is ample time for the cells to repair IR-induced DNA damage [Ljungman, 1999] supported here by the observation that CHK1 phosphorylation is eliminated by 24 hr after IR (Fig. 6). CHK1 phosphorylation after IR requires both ATR and ATM, with a peak of activation at 30-min postirradiation in hTERT-immortalized fibroblasts [Zhao and Piwnica-Worms 2001; Gatei et al., 2003]. Our observation that IR-induced CHK1 phosphorylation is decreased when cells are trypsinized is consistent with the model that trypsinizing and replating cells causes them to re-enter the cell cycle and resume DNA replication, which increases the likelihood of replication forks encountering an IR-induced lesion. Alternatively, it is known that trypsinization of cultured cells results in proteome changes [Huang et al., 2010]. It is possible that trypsinization immediately after irradiation disrupts the cell's ability to repair IR-induced damage, resulting in aberrant repair of lesions leading to CNVs. However, such lesions would be expected to be randomly distributed across the genome, as discussed above.

What is the nature of the IR-induced damage that leads to replication stress, and in turn CNVs? One possibility is that the combination of replication reentry and the resistance to further cell cycle delay makes IR-treated cells prone to replication-based DNA rearrangements, such as would occur when forks encounter SSBs or base damage, which occur frequently after IR [Ward, 1988]. It is known that IR induces SSBs at a frequency of about 1000 SSBs per cell per Gy and that these lesions can induce replication fork collapse [Kuzminov, 2001; Saleh-Gohari et al., 2005; Helleday et al., 2007; Harper et al., 2010]. These collapsed forks must undergo repair and then restart for replication to proceed to completion, and an inaccurate restart via a template switch mechanism such as MMBIR would be predicted to give rise to CNVs [Hastings et al., 2009].

It is interesting to note that, while most CNV hotspots are conserved after IR and replication stress, some APH/HU-induced deletion hotspots are duplication hotspots after IR. In particular, we note that these duplicated regions are physically shifted from the deletion regions within the same hotspot (Fig. 3B). This observation suggests that the mechanisms underlying deletions and duplications in these regions are different. A possible model to explain these differences involves single- versus double-fork failure and is illustrated in Figure 7. In the presence of global replication stress, each active fork is affected, increasing the likelihood of a double-fork failure. If two forks collapse while approaching one another, both forks will need to be repaired and restarted. A single MMBIR event could occur across both forks to restart replication, resulting in the deletion of intervening sequence. Such double-fork failures would be expected to occur more often when cells experience exogenous replication stress, as all forks would be impacted. In contrast, random damage caused by IR would more likely result in single-fork failure, if the lesion burden were low. If a collapsed fork does not have another nearby fork to use as an MMBIR target, it would instead need to find another region to serve as the template switch site. If MMBIR results in a jump to a region that has already been replicated, it

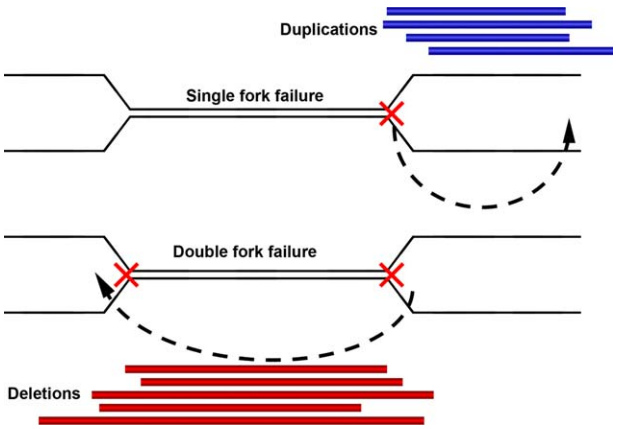

Fig. 7. Model of physically shifted deletion and duplication formation via single- and double-fork failure. When two nearby replication forks collapse (bottom), as might occur during global replication stress, MMBIR can occur between the two forks to restart replication, resulting in the deletion of intervening DNA (red bars). In the event of a single-fork failure (top), the absence of a nearby collapsed fork results in an MMBIR event into a nearby, already-replicated region, resulting in a duplication (blue bars). [Color figure can be viewed in the online issue, which is available at wileyonlinelibrary.com.]

would result in a duplication. Such a "backwards" jump might even preferentially occur if the downstream, active fork is creating supercoiled DNA ahead of it, which could make it a difficult region to invade.

It is also possible that the replication stress resulting after IR is not lesion driven but a result of altered checkpoint signaling, gene expression, or other factors in a global response. Such factors might include altered utilization of origins, especially dormant origins fired in response to stalled replication forks, or a general alteration in the progression rates of forks. Such a global alteration of replication dynamics could readily explain why IR CNVs occurred at the same hotspots as APH and HU CNVs, since these regions are clearly highly sensitive to inhibition of replication [Arlt et al., 2011b], even if the underlying reason in not yet known. The potential signal mediating a global IR effect is unknown, but could include the checkpoint activity evident in Figure 6.

In summary, we have shown that IR induces de novo CNVs via a mechanism similar to that in CNVs induced by APH and HU. A number of these CNVs occur in genes that have similar CNVs in genetic disease and cancer, such as *AUTS2* and *CDKN2A*. Such rearrangements could be due to collapse of forks encountering damage, altered replication origin usage or progression dynamics, or a combination of these factors. The susceptibility to IR-induced CNVs of cells undergoing DNA replication indicates that dividing tissues are at increased risk for this type of structural rearrangement. The observation that multiple exogenous agents lead to CNVs via a replication stress mechanism defines a class of CNV mutation, and predicts that any DNA damaging agent that interferes with replication is capable of creating such CNVs via this mechanism.

ACKNOWLEDGMENTS

The authors thank Mats Ljungman and James Tucker for insightful discussions and comments on the manuscript. They also thank Robert Lyons in the University of Michigan DNA Sequencing Core for providing Sanger sequencing.

AUTHOR CONTRIBUTIONS

MFA analyzed the data and prepared the manuscript. MFA, TEW, and TWG designed the study. SR, SRB, and MFA were responsible for data generation and data interpretation. MFA, SR, SRB, TEW, and TWG were involved in manuscript editing.

REFERENCES

Arlt MF, Mulle JG, Schaibley VM, Ragland RL, Durkin SG, Warren ST, Glover TW. 2009. Replication stress induces genome-wide copy number changes in human cells that resemble polymorphic and pathogenic variants. Am J Hum Genet 84:339–350.

Arlt MF, Ozdemir AC, Birkeland SR, Lyons RH Jr, Glover TW, Wilson TE. 2011a. Comparison of constitutional and replication stress-induced genome structural variation by SNP array and mate-pair sequencing. Genetics 187:675–683.

Arlt MF, Ozdemir AC, Birkeland SR, Wilson TE, Glover TW. 2011b. Hydroxyurea induces de novo copy number variants in human cells. Proc Natl Acad Sci USA 108:17360–17365.

Arlt MF, Rajendran S, Birkeland SR, Wilson TE, Glover TW. 2012. De novo CNV formation in mouse embryonic stem cells occurs in the absence of Xrcc4-dependent nonhomologous end joining. PLoS Genet 8:e1002981.

Beunders G, Voorhoeve E, Golzio C, Pardo LM, Rosenfeld JA, Talkowski ME, Simonic I, Lionel AC, Vergult S, Pyatt RE, et al. 2013. Exonic deletions in AUTS2 cause a syndromic form of intellectual disability and suggest a critical role for the C terminus. Am J Hum Genet 92:210–220.

Bignell GR, Greenman CD, Davies H, Butler AP, Edkins S, Andrews JM, Buck G, Chen L, Beare D, Latimer C, et al. 2010. Signatures of mutation and selection in the cancer genome. Nature 463:893–898.

Birkeland SR, Jin N, Ozdemir AC, Lyons RH Jr, Weisman LS, Wilson TE. 2010. Discovery of mutations in Saccharomyces cerevisiae by pooled linkage analysis and whole-genome sequencing. Genetics 186:1127–1137.

Carvalho CM, Pehlivan D, Ramocki MB, Fang P, Alleva B, Franco LM, Belmont JW, Hastings PJ, Lupski JR. 2013. Replicative mechanisms for CNV formation are error prone. Nat Genet 45:1319–1326.

Di Leonardo A, Linke SP, Clarkin K, Wahl GM. 1994. DNA damage triggers a prolonged p53-dependent G1 arrest and long-term induction of Cip1 in normal human fibroblasts. Genes Dev 8:2540–2551.

Dimitrijevic-Bussod M, Balzaretti-Maggi VS, Gadbois DM. 1999. Extracellular matrix and radiation G1 cell cycle arrest in human fibroblasts. Cancer Res 59:4843–4847.

Durkin SG, Ragland RL, Arlt MF, Mulle JG, Warren ST, Glover TW. 2008. Replication stress induces tumor-like microdeletions in *FHIT*/FRA3B. Proc Natl Acad Sci USA 105:246–251.

Gadbois DM, Bradbury EM, Lehnert BE. 1997. Control of radiation-induced G1 arrest by cell-substratum interactions. Cancer Res 57: 1151–1156.

Gadbois DM, Crissman HA, Nastasi A, Habbersett R, Wang SK, Chen D, Lehnert BE. 1996. Alterations in the progression of cells through the cell cycle after exposure to alpha particles or gamma rays. Radiat Res 146:414–424.

Gatei M, Sloper K, Sorensen C, Syljuasen R, Falck J, Hobson K, Savage K, Lukas J, Zhou BB, Bartek J, et al. 2003. Ataxia-telangiectasia-mutated (ATM) and NBS1-dependent phosphorylation of Chk1 on Ser-317 in response to ionizing radiation. J Biol Chem 278:14806–14811.

Glessner JT, Wang K, Cai G, Korvatska O, Kim CE, Wood S, Zhang H, Estes A, Brune CW, Bradfield JP, et al. 2009. Autism genome-wide copy number variation reveals ubiquitin and neuronal genes. Nature 459:569–573.

Guadagno TM, Assoian RK. 1991. G1/S control of anchorage-independent growth in the fibroblast cell cycle. J Cell Biol 115: 1419–1425.

Harper JV, Anderson JA, O'Neill P. 2010. Radiation induced DNA DSBs: Contribution from stalled replication forks? DNA Repair (Amst) 9:907–913.

Hastings PJ, Ira G, Lupski JR. 2009. A microhomology-mediated break-induced replication model for the origin of human copy number variation. PLoS Genet 5:e1000327.

Helleday T, Lo J, van Gent DC, Engelward BP. 2007. DNA double-strand break repair: from mechanistic understanding to cancer treatment. DNA Repair (Amst) 6:923–935.

Huang HL, Hsing HW, Lai TC, Chen YW, Lee TR, Chan HT, Lyu PC, Wu CL, Lu YC, Lin ST, et al. 2010. Trypsin-induced proteome alteration during cell subculture in mammalian cells. J Biomed Sci 17:36.

Karlsson R, Graae L, Lekman M, Wang D, Favis R, Axelsson T, Galter D, Belin AC, Paddock S. 2012. MAGI1 copy number variation in bipolar affective disorder and schizophrenia. Biol Psychiatry 71:922–930.

Kent WJ, Sugnet CW, Furey TS, Roskin KM, Pringle TH, Zahler AM, Haussler D. 2002. The human genome browser at UCSC. Genome Res 12:996–1006.

Kohno T, Yokota J. 2006. Molecular processes of chromosome 9p21 deletions causing inactivation of the p16 tumor suppressor gene in human cancer: deduction from structural analysis of breakpoints for deletions. DNA Repair (Amst) 5:1273–1281.

Kresse SH, Ohnstad HO, Paulsen EB, Bjerkehagen B, Szuhai K, Serra M, Schaefer KL, Myklebost O, Meza-Zepeda LA. 2009. LSAMP, a novel candidate tumor suppressor gene in human osteosarcomas, identified by array comparative genomic hybridization. Genes Chromosomes Cancer 48:679–693.

Krishnamoorthy K, Thomson J. 2004. A more powerful test for comparing two Poisson means. J Stat Plan Inference 119:23–35.

Kuzminov A. 2001. Single-strand interruptions in replicating chromosomes cause double-strand breaks. Proc Natl Acad Sci USA 98: 8241–8246.

Ljungman M. 1999. Repair of radiation-induced DNA strand breaks does not occur preferentially in transcriptionally active DNA. Radiat Res 152:444–449.

Pasic I, Shlien A, Durbin AD, Stavropoulos DJ, Baskin B, Ray PN, Novokmet A, Malkin D. 2010. Recurrent focal copy-number changes and loss of heterozygosity implicate two noncoding RNAs and one tumor suppressor gene at chromosome 3q13.31 in osteosarcoma. Cancer Res 70:160–171.

Saleh-Gohari N, Bryant HE, Schultz N, Parker KM, Cassel TN, Helleday T. 2005. Spontaneous homologous recombination is induced by collapsed replication forks that are caused by endogenous DNA single-strand breaks. Mol Cell Biol 25:7158–7169.

Ward JF. 1988. DNA damage produced by ionizing radiation in mammalian cells: identities, mechanisms of formation, and reparability. Prog Nucleic Acid Res Mol Biol 35:95–125.

Zhang F, Gu W, Hurles ME, Lupski JR. 2009. Copy number variation in human health, disease, and evolution. Annu Rev Genomics Hum Genet 10:451–481.

Zhao H, Piwnica-Worms H. 2001. ATR-mediated checkpoint pathways regulate phosphorylation and activation of human Chk1. Mol Cell Biol 21:4129–4139.